



Lawrence Berkeley Laboratory

UNIVERSITY OF CALIFORNIA

RECEIVED
LAWRENCE
BERKELEY LABORATORY

FEB 22 1982

LIBRARY AND
DOCUMENTS SECTION

ENERGY & ENVIRONMENT DIVISION

Submitted for the Proceedings of the Conference on
Large Body Impacts and Terrestrial Evolution:
Geological, Climatological and Biological Implications,
Snowbird, UT, October 19-22, 1981

GEOCHEMICAL ANOMALIES NEAR THE EOCENE-OLIGOCENE
AND PERMIAN-TRIASSIC BOUNDARIES

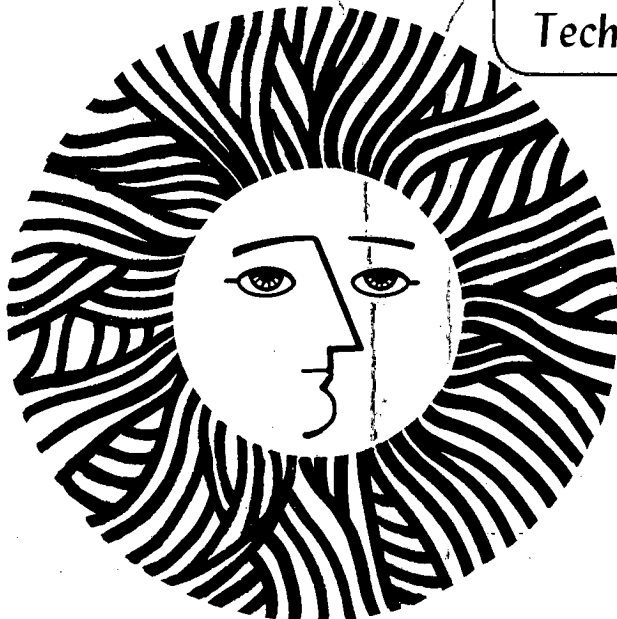
F. Asaro, L.W. Alvarez, W. Alvarez,
and H.V. Michel

October 1981

TWO-WEEK LOAN COPY

*This is a Library Circulating Copy
which may be borrowed for two weeks.*

*For a personal retention copy, call
Tech. Info. División, Ext. 6782*



LBL-13904
v.2

DISCLAIMER

This document was prepared as an account of work sponsored by the United States Government. While this document is believed to contain correct information, neither the United States Government nor any agency thereof, nor the Regents of the University of California, nor any of their employees, makes any warranty, express or implied, or assumes any legal responsibility for the accuracy, completeness, or usefulness of any information, apparatus, product, or process disclosed, or represents that its use would not infringe privately owned rights. Reference herein to any specific commercial product, process, or service by its trade name, trademark, manufacturer, or otherwise, does not necessarily constitute or imply its endorsement, recommendation, or favoring by the United States Government or any agency thereof, or the Regents of the University of California. The views and opinions of authors expressed herein do not necessarily state or reflect those of the United States Government or any agency thereof or the Regents of the University of California.

Geochemical Anomalies near
the Eocene-Oligocene and Permian-
Triassic Boundaries

F. Asaro*

L.W. Alvarez**,**

W. Alvarez***

H.V. Michel*

Paper submitted to the Proceedings of the Conference of Large Body
Impacts and Terrestrial Evolution: Geological, Climatological and
Biological Implications.

Snowbird Utah, Oct 19-22 1981

* Lawrence Berkeley Laboratory, University of California

** Space Sciences Laboratory, University of California at Berkeley

*** Department of Geology and Geophysics, University of California
at Berkeley.

This work was done with support from the Department of Energy under Contract
No. W-7405-ENG-48, the California Space Institute under Award CS24-81 and the
NASA Ames Research Center under Contract A-71683 B.

Iridium and other siderophile elements depleted in the earth's crust occur in anomalously high concentrations at the same stratigraphic level as the marine micropaleontological extinctions that define the Cretaceous-Tertiary boundary at about 66.7 m.y.B.P. This anomaly has been found worldwide and in both marine and terrestrial sediments. Geochemical details indicate the anomaly was caused by impact on the earth of an extraterrestrial object, probably having the composition of a carbonaceous chondrite and a diameter of about 10 km. A summary of the evidence supporting the impact theory is presented in another paper in these proceedings. (W. Alvarez and others, 1982)

The impact hypothesis for the terminal Cretaceous extinctions suggests that evidence for impact of an extraterrestrial object might be found at the stratigraphic horizons of other mass extinctions. In fact, there is already one case where evidence for an impact is known at, or at least close to, such a horizon. The North American tektites on land and the associated microtektites studied in sea-bottom cores provide direct evidence for a major impact (B.P. Glass and others, 1973, 1979a, 1979b; F. Murrasse and B.P. Glass, 1976). The strewnfield extends halfway around the earth and contains at least 10^{10} metric tons of impact melt in the form of far-traveled glassy spherules (B.P. Glass and others, 1979b). Five radiolarian species die out at the microtektite level (B.P. Glass and others 1979a), but the event occurred about 2 m.y. (B.P. Glass and J.R. Crosbie, 1981) before the Eocene-Oligocene boundary as defined in the Deep-Sea Drilling Project (DSDP) reports (N.T. Edgar and others, 1973). The boundary defined in this way may or may not be synchronous with the major turnover of mammal taxa that defines the Eocene-Oligocene boundary in terrestrial sequences in North America,

Europe, and Asia (M. Brunet, 1977; D.E. Savage, 1981), a question beyond the scope of this paper. Data from Brunet are shown in Fig. 1. Dates suggested for the boundary are 32.5 ± 0.9 m.y. (B.P. Glass and J.R. Crosbie, 1981) and 38.0 m.y. (G. Ness and others, 1980). The best value for the fission track and K/Ar ages of North American tektites is $34.2 \pm .6$ m.y. (B.P. Glass and J.R. Crosbie, 1981), and the microtektites give fission track ages of 34.6 ± 4.2 m.y. (B.P. Glass and others, 1973).

The possible relation between the Eocene-Oligocene extinctions and a major impact has been considered by others (H.C. Urey, 1973; B.P. Glass and others, 1979b, J.A. O'Keefe, 1980). In order to determine whether the impact that produced the North American strewnfield also gave rise to an iridium anomaly, we measured the abundances of many elements by high-precision techniques (I. Perlman and F. Asaro, 1969, 1971; F. Asaro and others, 1981a; F.H. Stross and others, 1981) of neutron activation analysis (NAA) in 9 samples from cores 30 and 31 of DSDP site 149 in the eastern Caribbean. The preliminary report on this work, including the recognition of a distinct iridium anomaly, appeared as an abstract in the program for this meeting (F. Asaro and others, 1981b).

DSDP site 149 cored a "radiolaria-rich nannoplankton chalk" in the Middle Oligocene of core 30, and "semi-indurated calcareous-rich radiolarian ooze" in the Upper Eocene of core 31 (N.T. Edgar and others, 1973). The basal Oligocene is missing between cores 30 and 31 (N.T. Edgar and others, 1973; F. Maurrasse, 1976) a gap possibly amounting to 7 m (B.P. Glass and others, 1979a). This was the discovery site for the North American microtektites (T.W. Donnelly and others), but unfortunately the peak of microtektite abundance was apparently lost in the

unrecovered interval between cores 30 and 31. The microtektite abundance rises rapidly at the top of core 31, but is back to near zero at the base of core 30 (Fig. 2). Despite the missing section, this core offered an opportunity to look for an extraterrestrial component.

Data for 33 elements are shown in Tables I-IV. Nearly all elements were calibrated vs. a secondary standard, STANDARD POTTERY (I. Perlman and F. Asaro, 1971). Calcium and Cl were calibrated vs. primary standards of CaCO_3 and KCl, respectively, and Ir was calibrated vs. a secondary standard, DINO-1 (prepared from the Danish Cretaceous-Tertiary boundary layer) with an Ir abundance of $31.5 \pm .6$ ppb. Recalibration of STANDARD POTTERY for Cr, Ni and Lu gave new values of 102 ± 4 , 278 ± 7 (H.V. Michel and F. Asaro, 1980), and $.425 \pm .016$ ppm (F. Asaro and others, ND), respectively. The precisions of measurement indicated in the tables are estimates of standard deviations. As the abundances of the elements in the secondary standards are accurately known, the accuracies of the data are comparable to the listed precisions. In neutron activation analyses the subtraction of gamma-ray backgrounds comparable to peak intensities sometimes results in negative differences. If a difference is small or negative only the upper limit is usually given. For Ir, however, negative or small differences are also given in parentheses.

Nearly all of the measured elements appear to correlate with (or be consistent with) Ca (probably reflecting CaCO_3 deposition), or Al (probably reflecting clay or other aluminum silicate deposition), or Sm (possibly reflecting phosphate deposition) or combinations of these. Examples of whole-rock and carbonate-free abundances are shown in Fig. 3 and

4, respectively. Fig. 5 shows rare earth patterns for some of the Oligocene and Late Eocene samples. The Ce depletion, which probably reflects the known Ce depletion in sea water (E.D. Goldberg and M. Koide, 1963), is more severe in the Late Eocene than in the Oligocene samples. This suggests a larger ratio of biogenic (e.g., phosphate) to detrital (e.g., clay) components in the former. If one element correlates with another, then their ratio of abundances should remain fairly constant for all or nearly all of the 9 samples. If one element, a, correlates with two others, b and c, then the abundance ratio a/b should be fairly linear with the ratio c/b for all or nearly all of the 9 samples. Ba correlates very poorly with the other elements possibly because it is the only element listed with a very insoluble sulphate. Ta and U correlate roughly with Al, but have one or two samples in poor agreement. Ta and Zn patterns are shown in Fig. 6. Zn and Ir do not correlate with any other element or with each other. The Zn cannot be due to the microtektites since they contain only ~150 ppm Zn (R.D. Giauque, 1981) as measured by x-ray fluorescence. As Zn is a common terrestrial element, Zn geochemical anomalies can have a variety of terrestrial sources. This is not, however, true of Ir.

Anomalously high iridium levels were found, coinciding with the highest abundance of microtektites, at the top of core 31. The two highest samples in core 31 have Ir concentrations of $.41 \pm .16$ and $.34 \pm .10$ ppb, as a fraction of the whole rock. The next lower sample has an Ir concentration which may follow the trend of the microtektite abundance but is also indistinguishable from zero (see Fig. 2). The other six samples, at levels where microtektites are very rare or absent, have Ir concentrations which are indistinguishable from zero and have a best

value of 0.00 ± 0.05 ppb. Fig. 7 demonstrates how an anomaly of about 0.4 ppb Ir can be determined by neutron activation analysis without chemical separations.

Discovery of the Late Eocene iridium anomaly raises a number of questions for further study, but a few preliminary considerations can be given here. Of the six Late Eocene samples, the two which definitely contain Ir average 34.5 ppm Cr and 92 ppm Ni, and the other 4 average slightly less. The maximum abundances of these elements which should be due to a separate component in the Ir-rich samples are 8.5 and 29 ppm, respectively, after statistical treatment of the data to provide about a 95% confidence level. Ultramafic rocks contain Ir in even higher abundances than the observed anomaly but estimates of their contribution can be made because of their high Cr and Ni contents. From 126 measurements in ultramafic rocks of Ni and Ir abundances (A.J. Naldrett and others, 1979; J.R. Ross and R.R. Keays, 1979; D.I. Groves and R.R. Keays, 1979) and 24 of Cr and Ir (D.I. Groves and R.R. Keays, 1979) the expected Ni and Cr abundances in the Ir-rich samples due to such an intrusion would average ~48 and 126 ppm respectively, much higher than the observed limits (if no marine fractionation is assumed). If, on the other hand, the intrusive component were due to a chondritic extraterrestrial source, the added Cr and Ni abundances would be ~2 and 7 ppm (B. Mason, 1971a) respectively, consistent with the observed limits.

Meteorite ablation debris is continually accumulating in deep-sea sediments. From the 1.6 mm/1000 yr sedimentation rate for the Late Eocene in DSDP site 149 (F. Maurrasse, 1976) and the relationship between Ir abundance and sedimentation rate (J.L. Barker, Jr. and E.

Anders, 1968), corrected for appropriate densities, the maximum expected Ir concentration would be 0.02 ppb. The observed value is 20 times higher, which agrees with the interpretation of the microtektites as evidence for a single large impact.

Measurements of Ir in the microtektites are in progress, but in the meantime, estimates are useful. If the Os abundance of ≤ 1 ppb in the correlative Bediasite tektite from Texas (J.H. Crocket, 1969), and the typical Ir/Os ratio of about 1 in chondritic material (B. Mason, 1971b) are combined with the maximum abundance of microtektite mass in core 31, 0.2% (B.P. Glass and M.J. Zwart, 1979a), the Ir abundance at the top of core 31 would be < 0.002 ppb. The much higher values observed indicate that the iridium was not carried primarily by the microtektites. This agrees with the interpretation that tektites are formed from shock-melted target rock, with only a minor contamination by extraterrestrial material.

The principal conclusions are first, that the association of iridium anomalies with major impact events, inferred for the Cretaceous-Tertiary boundary, is strengthened by recognition of an iridium anomaly at a microtektite horizon; second, although not all impacts which produce detectable iridium enrichments are necessarily related to extinctions (F.T. Kyte and others, 1981), the association of iridium anomalies with extinctions is strengthened by the synchronous disappearance of 5 species of radiolaria with the appearance of the iridium and microtektite anomalies near the Eocene-Oligocene boundary; and third, that detailed studies of the latest Eocene are needed to determine whether or not the terminal Eocene mass extinction of land mammals is synchronous

with the tektite-iridium horizon.

About 230 million years ago at the boundary between the Permian and Triassic periods, there were mass extinctions which have been considered at least comparable to those at the end of the Cretaceous Period. In order to assist in a search for geochemical anomalies which might be associated with the Permian-Triassic (P-T) boundary, John Utting (of the department of Geological Research and Services of Petro-Canada in Calgary) kindly provided samples and site descriptions from two sections about 1300 km apart in the Peoples Republic of China. These were the Tien Bao section near Pao Ching village near Nanjing and the Wachapo Mountain section near Wanching Luco village about 10 km northwest of Kweiyang in Kweichow Province. Through the kind assistance of Fang Yi, who was Minister in Charge, The State Scientific and Technological Commission of the Peoples Republic of China, and Frank Press, Scientific Advisor to President Carter, a suite of samples was recently obtained from the Tangshan section about 20-25 km east of Nanjing. These samples were collected by Lung S. Chan (U.C. Berkeley) with the guidance of Lin Rui, research geologist in the Nanjing Institute of Geology and Paleontology, Academia Sinica. As data are still being taken on this latter suite of samples, only fragmentary information can be given.

Eleven samples were measured from the Tien Bao section. Six of these came from a mudstone unit of the Chinglung Formation (basal Triassic) which had a thin clay layer at the bottom, and five came from the Changhsing Formation (latest Permian) which is a well-bedded limestone with thin shale beds. Two samples were measured from Wachapo Mountain. One was clay from 6 inches above the P-T boundary in the Teiyeh Forma-

tion (basal Triassic), and the other was shale from 2 feet below the boundary in the Changhsing Formation. The abundances of 25 elements were measured by techniques of neutron activation analysis previously described, and the data are shown in Tables V and VI. In Fig. 8 are shown selected carbonate-free mean abundances for groups of Triassic, boundary (lowest Triassic) and Permian samples from the Tien Bao section. The large difference in chemical abundances between the boundary samples and those above and below is obvious. Comparably high abundances of Th, Ta and Hf and the very low values for Cr were also found in the P-T boundary in the Tangshan section near Nanjing (not shown in the Tables) and at Wachapo Mountain, 1300 km away. The similarities of these rather unusual abundances in clay at these three location strongly suggest a common origin.

It was previously known that the Tien Bao and Wachapo Mountain boundary layers contained smectite. (J. Utting, 1980) Miriam Kastner (1982) from the University of California at San Diego has made an x-ray diffraction study of two P-T boundary clays from the Tangshan section as well as two Triassic samples (from 0-2 and 8-10 cm above the boundary) and three Permian samples (from 0-4, 8-10 and 30 cm below the boundary). The boundary samples were different from all of the others in that they were predominantly (85-95%) a mixed-layer smectite/illite clay. All of the other samples contained principally quartz, feldspar and illite. They also contained some of the mixed-layer clay although it was not a major phase. Kastner stated the mixed-layer clay is most likely the alteration product of a pure smectite which itself was the alteration product of a glass. The proportion of illite layers in the mixed-layer smectite/illite clay is 50-60%. Aging increases the relative amount of

illite layers, and Kastner found the measured value to be quite consistent with the known age of the sediments.

Thus both the recent chemical and x-ray diffraction evidence support the conclusion that the P-T boundary layer has a different origin than the sediments above and below. If this layer was originally glass, it could have originated from volcanism or the result of the impact of an extraterrestrial object. In the latter explanation Ir should be associated with the boundary layer. Measurements of the Tien Bao and Wachapo Mountain sections showed no detectable iridium with an upper limit of ~0.5 ppb. A measurement of the Tangshan section also showed no detectable Ir with an upper limit of .055 ppb. From the available data, a volcanic origin for the measured boundary clay appears the most likely, although an extraterrestrial impact cannot be ruled out. A comet, with an impact velocity possibly 5 times higher than that of earth-crossing asteroids and a head consisting roughly of half ice and half chondritic material could produce an explosion comparable to that envisioned as the cause of the Cretaceous-Tertiary extinctions, if its mass was less than the canonical 10 km diameter asteroid by a factor of $5^2 \times 2 = 50$. Therefore, it would be expected to contribute about 2% as much Ir to the P-T boundary as an asteroid would have contributed to the C-T boundary. In order to check this latter possibility further improvements in chemical technique are being made to obtain better sensitivity for iridium.

We are very grateful to Frank Press and Fang Yi, Vice Consul of China, for their help in arranging for the procurement of P-T rock samples. We appreciate the efforts of Lung S. Chan of U.C. Berkeley, Lin

Rui of the Academia Sinica and John Utting in the collection of P-T rock samples. We are very much indebted to Miriam Kastner for the x-ray diffraction study and to Robert Giaque for the x-ray fluorescence measurements. We are very thankful to B.P. Glass and D.E. Savage for helpful discussions. Neutron irradiations were kindly provided by Tek Lim, supervisor of the small U.C. Berkeley research reactor, and his staff.

This work was done with support from the Department of Energy under Contract W-7405-ENG-48, the California Space Institute under Award CS24-81 and the NASA Ames Research Center under Contract A-71683 B. The DSDP samples were supplied through the assistance of the National Science Foundation.

- Alvarez, W., Alvarez, L.W., Asaro, F. and Michel, H.V., 1982, Current Status of the Impact Theory for the Terminal Cretaceous Extinction: Proceedings of the Conference on Large Body Impacts and Terrestrial Evolution: Geological, Climatological and Biological Implications.
- Asaro, F., Bowman, H.R. and H.V. Michel, ND, unpublished data .
- Asaro, F., Michel, H.V. and Burger, R.L., 1981a, Chemical Source Groups in Ecuadorian Obsidian: Lawrence Berkeley Laboratory Preprint LBL-13247 (September).
- Asaro, F., Alvarez, L.W., Alvarez, W. and Michel, H.V., 1981b, Geochemical anomalies near the Eocene-Oligocene and Permian-Triassic boundaries: Abstracts for the papers to the Conference on Large Body Impacts and Terrestrial Evolution: Geological, Climatological, and Biological Implications, p.2.
- Barker, J.L., Jr., and Anders, E., 1968, Accretion rate of cosmic matter from iridium and osmium contents of deep-sea sediments: *Geochemica et Cosmochimica Acta*, v.32 p. 627-645.
- Brunet, M. 1981, Les Mammifères et le problème de la limite Eocene-Oligocene en Europe: *Geobios, Mémoire Spécial*, v.1, p. 11-27.
- Crocket, J.H., 1969, Platinum metals: Handbook of Geochemistry, II-1, 78-C-21, edited by K.H. Wedepohl, published by Springer-Verlag, New York.
- Cullers, R., Chaudhuri, S. Kilbane, N., and Koch, R., 1979, Rare-earth elements in size fractions and sedimentary rocks of Pennsylvanian-Permian age from the mid-continent of the U.S.A.: *Cosmochimica et Geochimica*

Acta, V. 43, p. 1285-1301.

Donnelly, T.W. and Chao, E.C.T., 1973, Microtektites of Late Eocene Age from the Eastern Caribbean Sea: Initial Reports of the Deep Sea Drilling Project, v. 15, p. 1031-1037.

Edgar, N.T., Saunders, J.B., Donnelly, T.W., Schneidermann, N., Maurrasse, F., Bolli, H.M., Hay, W.W., Reidel, W.R., Premoli Silva, I., Boyce, R.E., and Prell, W., Site 146/149: Initial Reports of the Deep Sea Drilling Project, v. 15, p. 130.

Giauque, R.D., 1981. Private communication to the authors.

Glass, B.P., Baker, R.N., Strozer, D. and Wagner, G.A., 1973, North American microtektites from the Caribbean Sea and their fission track ages: Earth and Planetary Science Letters, v. 19, p. 184-192.

Glass, B.P., and Zwart, M.J., 1979a, North American microtektites in Deep Sea Drilling Project cores from the Caribbean Sea and Gulf of Mexico: Geological Society of America Bulletin, Part I, v. 90, p. 595-602.

Glass, B.P., Swincki, M.B. and Zwart, P.A., 1979b, Australasian, Ivory Coast, and North American tektite strewnfields: Size, mass and correlation with geomagnetic reversals and other earth events: Proceedings of the 10th Lunar and Planetary Science Conference, p. 2535-2545.

Glass, B.P., and Crosbie, J.R., 1981, Age of the Eocene-Oligocene boundary based on extrapolation from the North American microtektite layer: Geological Society of America, Abstracts with Programs, v.13, p. 460.

- Goldberg, E.D. and Koide, M., 1963, Rare-Earth Distributions in the Marine Environment: *Journal of Geophysical Research*, V. 68, p. 4209-4217.
- Groves, D.I. and Keays, R.R., 1979, Mobilization of elements during alteration of dunites, Mt. Keith-Betheno, Western Australia: *Canadian Mineralogist*, v. 17, p. 373-389.
- Kastner, M., 1982, private communication to F. Asaro.
- Kyte, F.T., Zhou, Z. and Wasson, J.T., 1981, High noble metal concentrations in a late Pliocene sediment: *Nature*, v. 292, p. 417-420.
- Mason, B., 1971a, Handbook of Elemental Abundances in Meteorites, Gordon and Breach Science Publishers, New York, p. 193, 221, and 463.
- Mason, B., 1971b, Handbook of Elemental Abundances in Meteorites, Gordon and Breach Science Publishers, New York, p. 451 and 463.
- Masuda, A., Nakamura, N. and Tanaka, T., 1973, Fine structures of mutually normalized rare-earth patterns of chondrites: *Geochimica et Cosmochimica Acta*, v. 37, p. 239-248.
- Maurrasse F. and Glass, B.P., 1976a, Radiolarian stratigraphy and North American microtektites in Caribbean RC9-58: implications concerning Late Eocene radiolarian chronology and the age of the Eocene-Oligocene boundary: *Transactions of the VII Caribbean Geological conference, French Antilles, June 30-July 12, 1974*, p. 205-212.
- Maurrasse, F., 1976b, Paleoecologic and paleoclimatic implications of radiolarian facies in Caribbean Paleogene deep-sea sediments: *Transac-*

tions of the VII Caribbean Geological Conference, French Antilles, June 30-July 12, 1974, 185-204.

Michel, H.V., and Asaro, F., 1980, unpublished data.

Naldrett, A.J., Hoffman, E.L., Green, A.H., Chou C. and Naldrett, S.R.,
The composition of Ni-sulfide ores, with particular reference to their
content of PGE and Au: Canadian Mineralogist, v. 17, p. 403-415.

Ness, G., Levi, S., and Couch, R., 1980, Marine magnetic anomaly time-
scales for the Cenozoic and Late Cretaceous: a précis, critique, and
synthesis, Reviews of Geophysics and Space Physics, v. 18, p. 753-770.

O'Keefe, J.A., 1980, The terminal Eocene event: formation of a ring sys-
tem around the Earth?, Nature, v. 285, p. 309-311.

Perlman, I. and Asaro, F., 1969, Pottery analysis by neutron activation:
Archaeometry, v. 11, p. 21-52.

Perlman, I., and Asaro, F., 1971, Pottery analysis by neutron activa-
tion: Science and Archaeology, edited by R.H. Brill, published by
M.I.T. Press, Cambridge, MA, p. 182-195.

Ross, J.R. and Keays, R.R., 1979, Precious metals in volcanic-type
nickel sulfide deposits in Western Australia I. Relationship with the
composition of the ores and host rocks: Canadian Mineralogist, v. 17,
p. 417-435.

Savage, D.E., 1981 private communication to W. Alvarez.

Stross, F.H., Sheets, P., Asaro, F. and Michel, H.V., 1981, Precise
characterization of Guatemalan obsidian sources and source

determinations of artifacts from Quirigua: Lawrence Berkeley Laboratory
Preprint LBL-12252 Revised (November), submitted to American Anti-
quity.

Urey, H.C., 1973, Cometary collisions and geological periods: Nature,
v. 242, p. 32-33.

Utting, J., 1980, private communication to W. Alvarez.

Figure Captions

Fig.1 Mammalian distribution at Eocene-Oligocene boundary in the Paris Basin.

Fig.2 Eocene-Oligocene geochemical anomalies in DSDP Site 149.

Fig.3 Selected whole-rock element abundances near the Eocene-Oligocene boundary in DSDP Site 149.

Fig.4 Selected element abundances near Eocene-Oligocene boundary in DSDP Site 149. Sea water contaminations have been removed, and the abundances have been recalculated on a calcium-carbonate-free basis.

Fig.5 Rare earth abundance patterns in Late Eocene and Oligocene sediments of DSDP Site 149. Eocene samples are from Intervals 1-2, 3-4, 14-15 and 84-85 cm below the top of Core 31 Section 1. Oligocene samples are from Intervals 20-21 and 140-141 cm below the top of Core 30 Section 2. The abundance of each element was normalized by dividing it by the abundance of that element in the chondritic Leedy meteorite (A. Masuda and others, 1973), and the resulting ratios were each divided by the equivalent Sm ratio. The error bars are root-mean-square deviations. The Ce depletion is estimated as the deviation from a straight-line dependence between La and Sm. Work on shales from Kansas and Oklahoma indicate this is a reasonable approximation (Cullers and others, 1979).

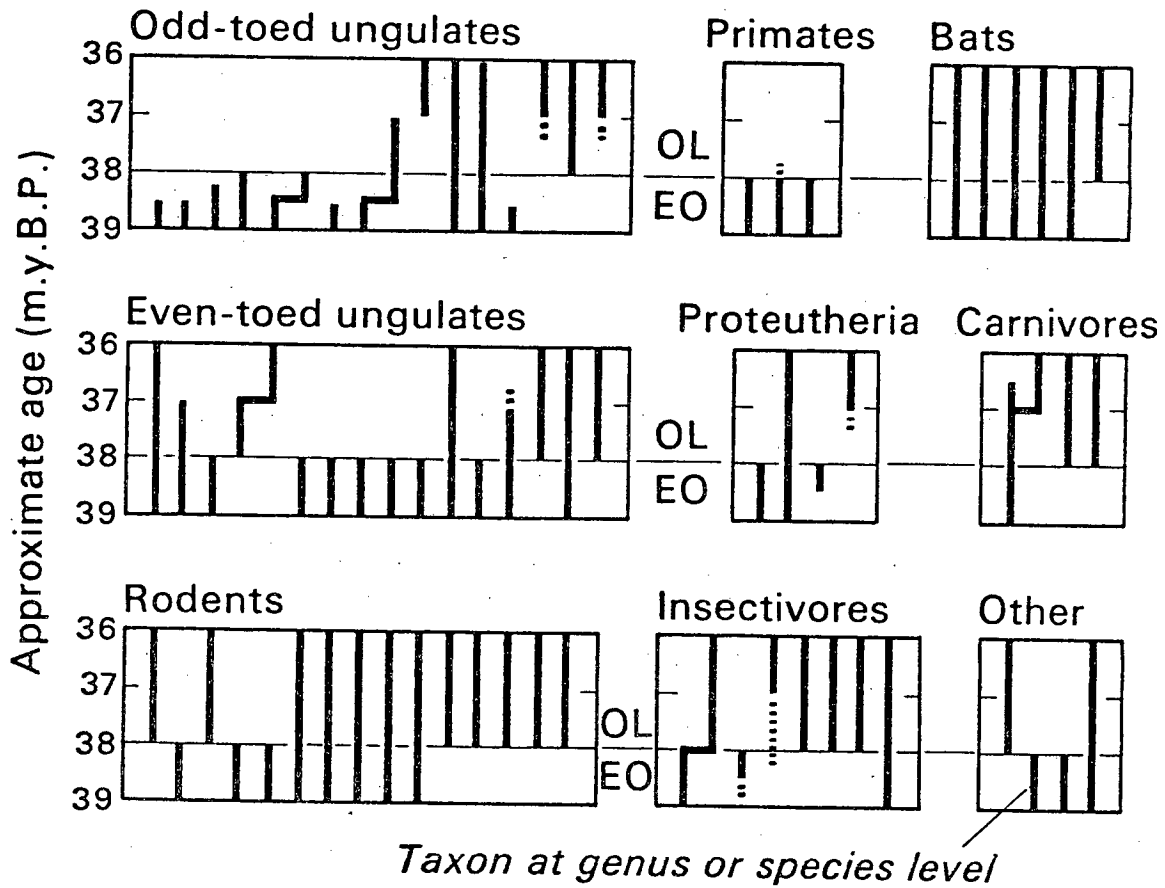
Fig.6 Unusual element abundance patterns near the Eocene-Oligocene boundary in DSDP Site 149. The abundances have been recalculated on a calcium-carbonate-free (and sea water-residue-free) basis. The Ta pattern is the same as that of Al except for a very high value at the top of Core 31.

Fig.7 Demonstration of the iridium anomaly near the Eocene-Oligocene boundary in DSDP Site 149. These are gamma-ray spectra in the region of the 468 Kev gamma ray of ^{192}Ir which were taken during a period of ~1-2.5 months after neutron irradiation of the samples. In order to minimize odd-even effects in the channels of the pulse-height analyzer, the channels are summed in pairs. The errors are standard deviations in the counting of gamma rays. The spectral interference due to ^{131}Ba was calculated from the abundance of other ^{131}Ba gamma rays and is shown as a bump in each of the solid curves. The spectral interference of Sb was calculated in a similar way, and those of ^{154}Eu and ^{140}Ba (from ^{235}U fission in the reactor) were determined from the measured Eu and U contents of the samples. The latter three interferences are shown by bumps in the solid curves of the two left spectra and in the dashed curves of the two right spectra. The steep rise at the highest energy of each spectrum is due to a minor gamma ray of ^{134}Cs . Upper left spectrum: sum of 858 min count on sample 2038-E and counts totaling 4874 min on 2038-F. Lower left spectrum: sum of counts totaling 3881 min on sample 2038-J and 3291 min on sample 2038-K. Upper right spectrum: sum of counts totaling 3018 min on sample 2038-G. Lower right spectrum: sum of counts totaling 8423 min on

2038-H.

Fig.8 Element abundances of P-T rocks from the Tien Bao section near Nanjing in the Peoples Republic of China. The abundances have been recalculated on a calcium-carbonate-free basis.

MAMMALIAN DISTRIBUTION AT EOCENE-OLIGOCENE BOUNDARY (Paris Basin)

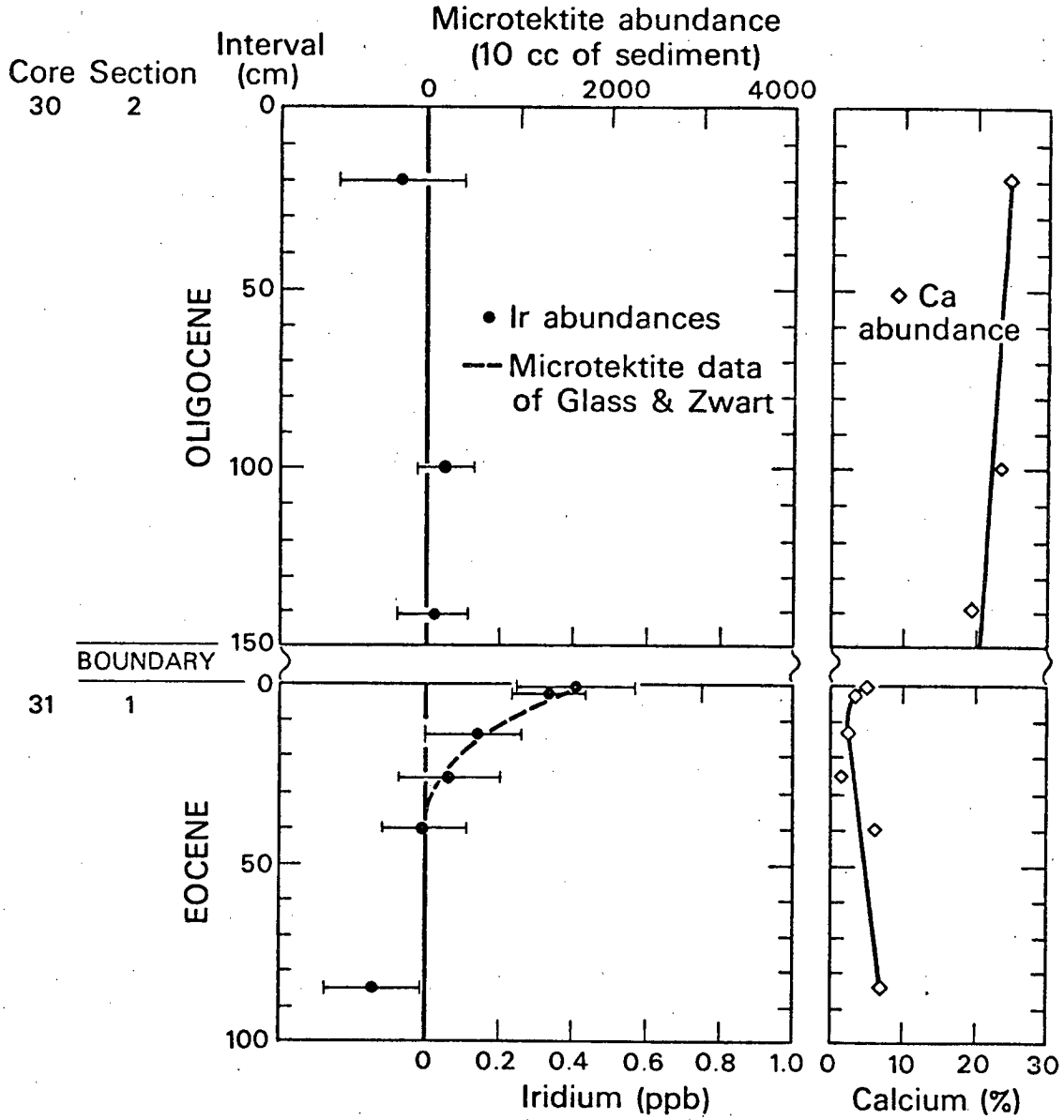


Data from M. Brunet (1977)

XBL 8110-1436

Figure 1

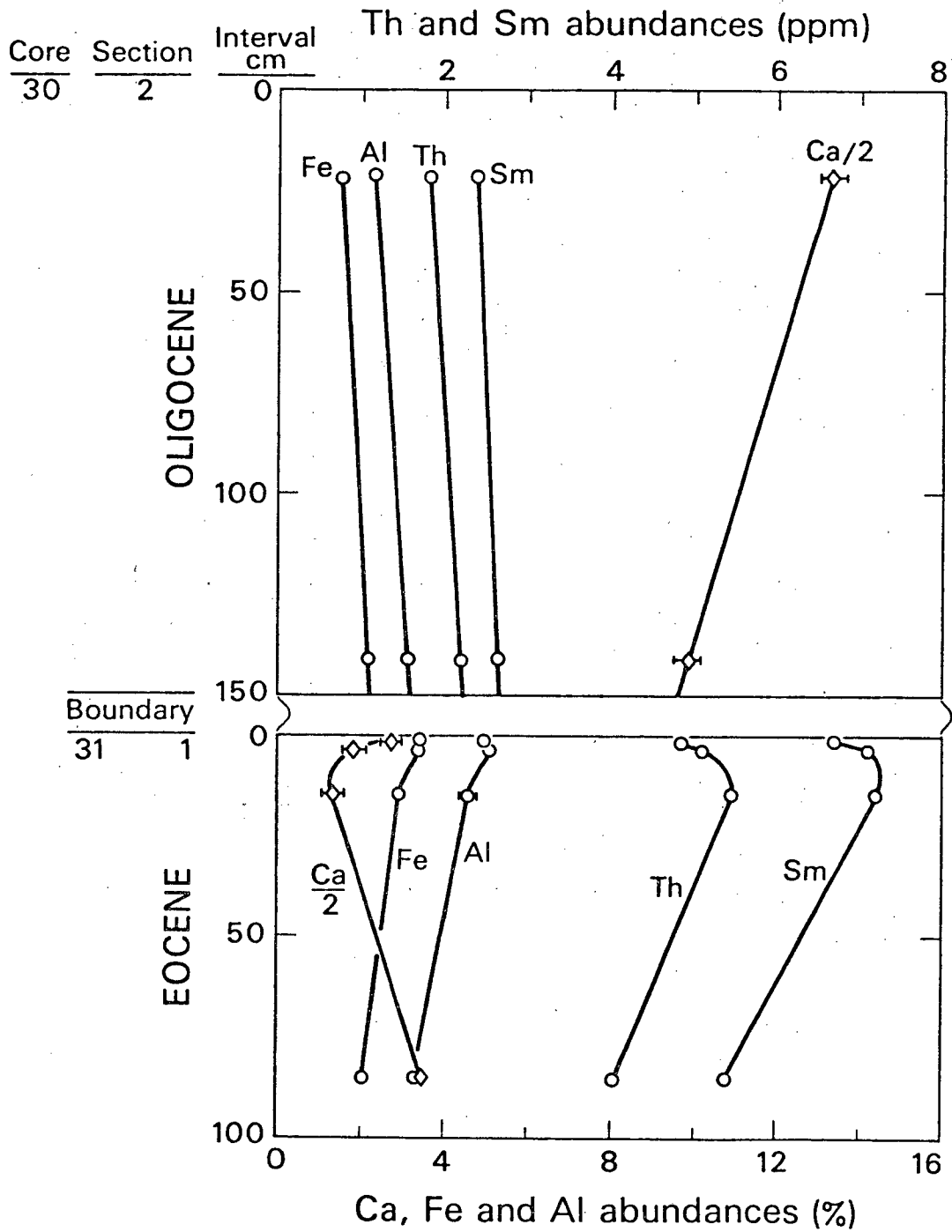
DSDP Site 149 EOCENE-OLIGOCENE GEOCHEMICAL ANOMALIES



XBL 819-1356

Figure 2

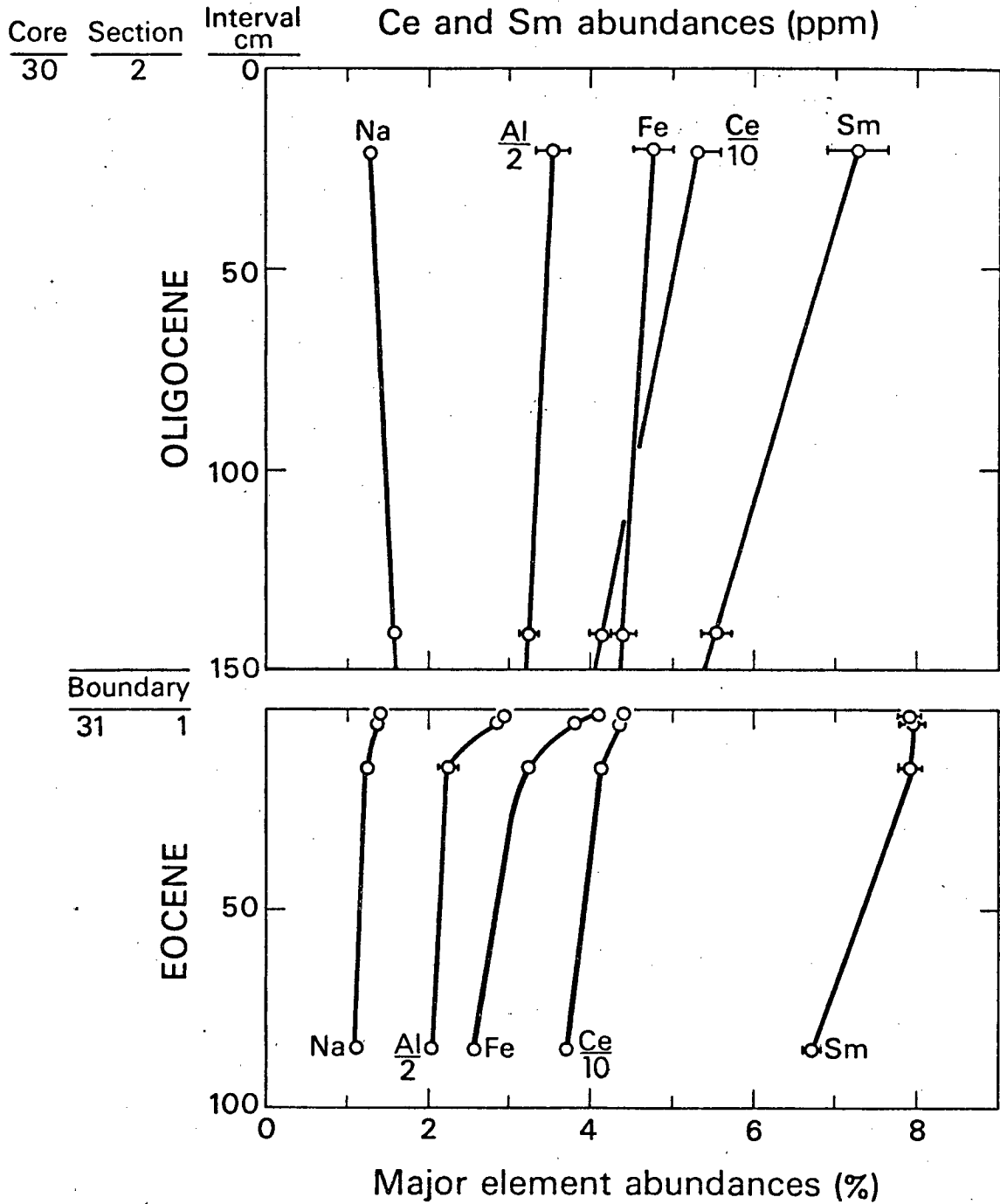
DSDP SITE 149 WHOLE-ROCK ELEMENT ABUNDANCES



XBL 8110-1425

Figure 3

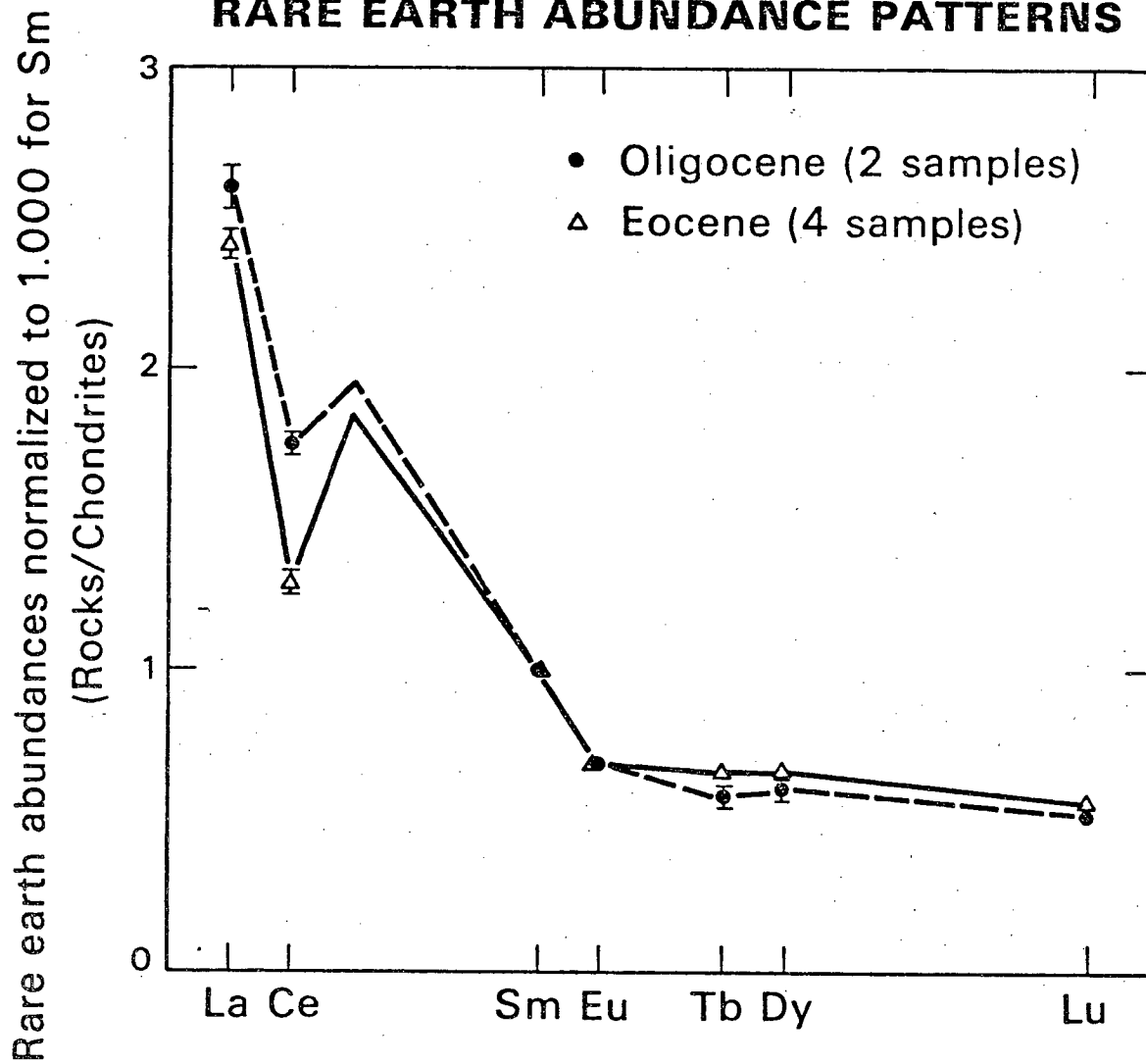
DSDP SITE 149 CARBONATE FREE ABUNDANCES



XBL 8110-1424

Figure 4

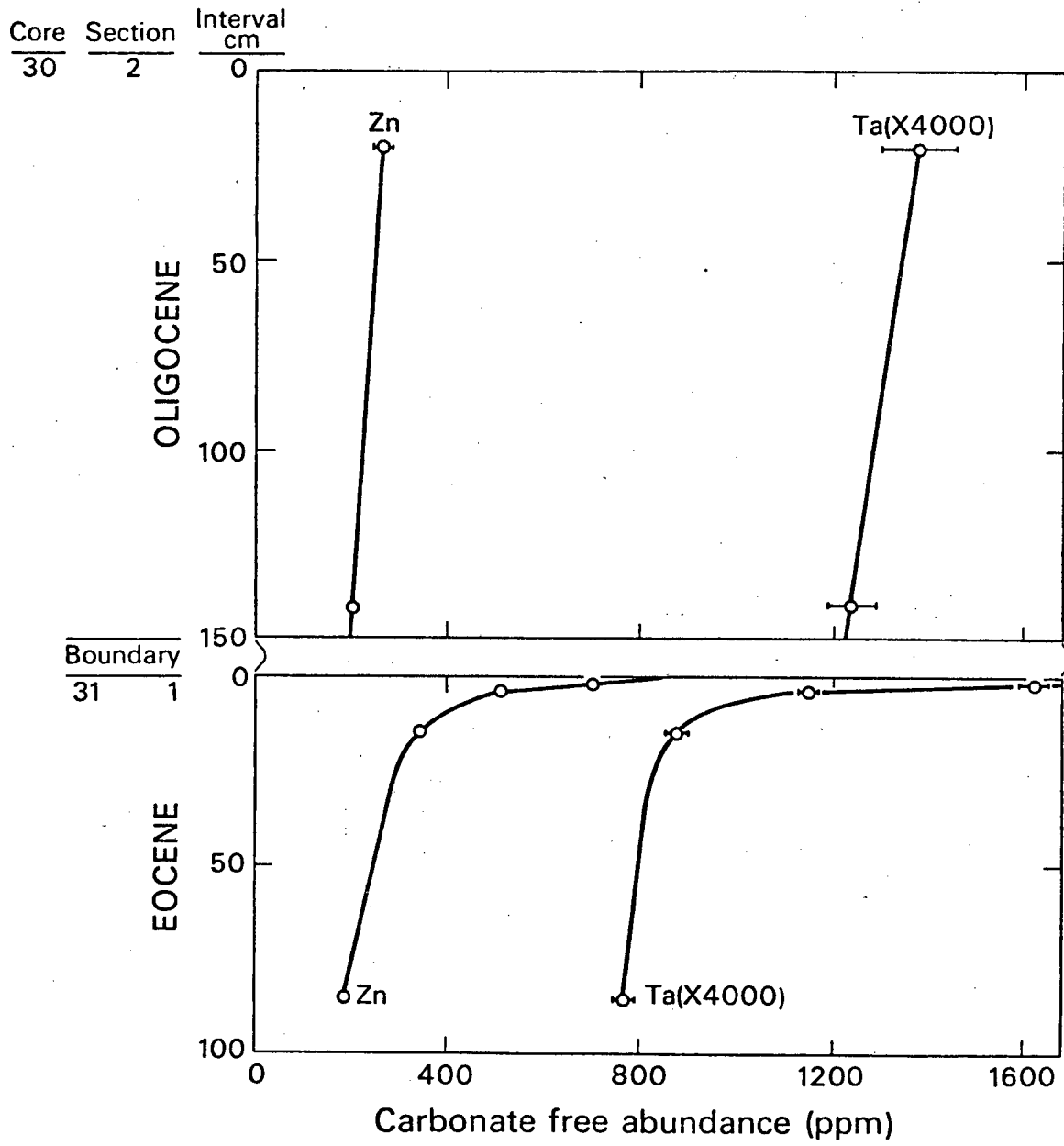
DSDP SITE 149 RARE EARTH ABUNDANCE PATTERNS



XBL 8110-1423

Figure 5

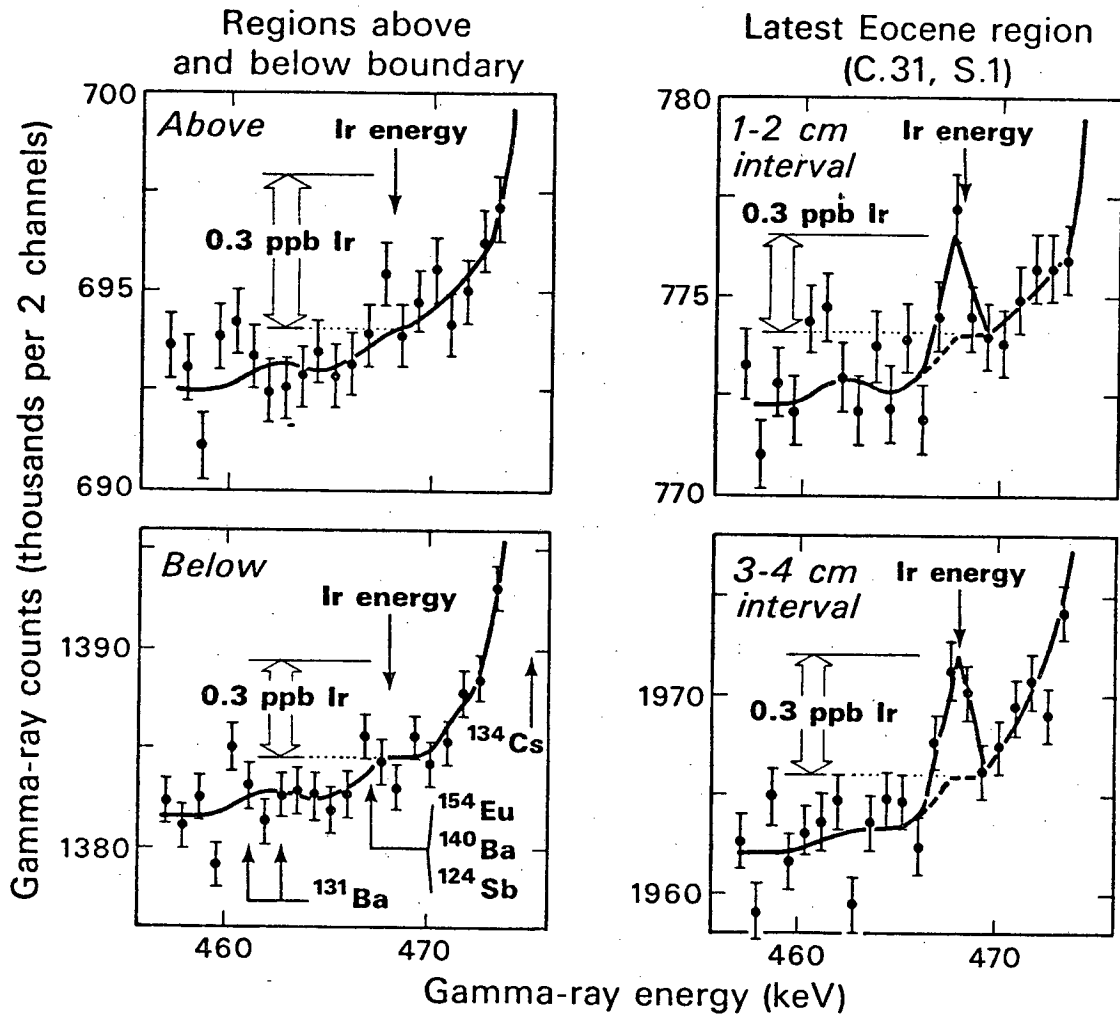
DSDP SITE 149 UNUSUAL ABUNDANCE PATTERNS



XBL 8110-1426

Figure 6

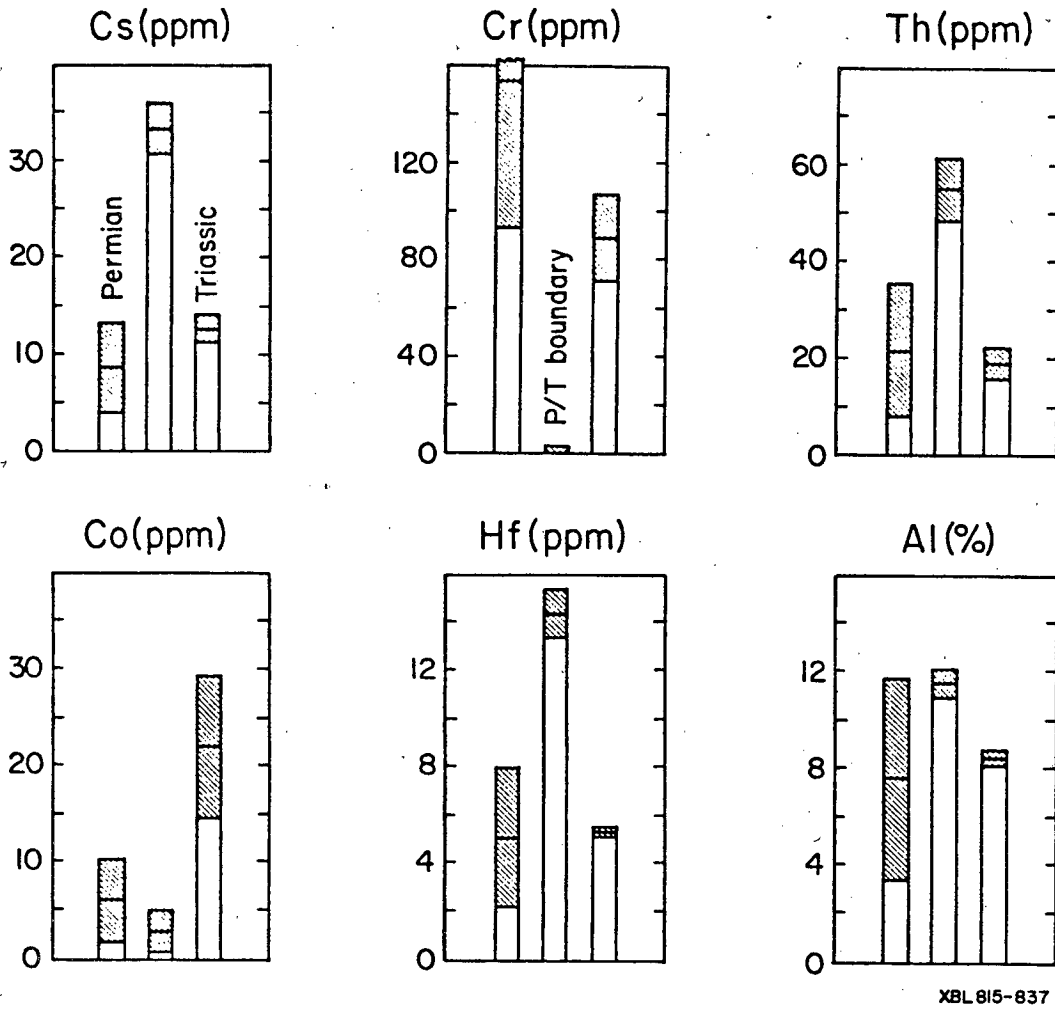
IRIDIUM ANOMALY NEAR EOCENE-OLIGOCENE BOUNDARY DSDP Site 149 (Caribbean Sea)



XBL 819-1357

Figure 7

Abundances in Permian-Triassic rocks from Nanking, China (Assumed carbonate-free basis)



XBL 815-837

Figure 8

TABLE I

Major element abundances (expressed in %) in

DSDP Site 149 near the Eocene-Oligocene boundary

Sample Name	NAA Pill	Core	Section	Interval (Cm)	Ca	Al	Cl	Na ¹	K	Mg ¹	Ti	Fe
DSEA-117	2038-E	30	2	20-21	25.1±.7	2.29±.05	.352±.030	.421±.021	<.6	<1.5	.096±.022	1.555±.019
-173	2045-X	30	2	100-101	23.5±.8	2.22±.06	1.131±.037	.601±.023	<.7	<1.6	.161±.037	1.553±.018
-118	2038-F	30	2	140-141	19.7±.7	3.09±.07	1.56±.04	.758±.039	<.6	1.6±.6	.140±.023	2.111±.025
-119	2038-G	31	1	1-2	5.4±.5	4.94±.11	.944±.034	1.199±.039	.73±.26	1.7±.6	.216±.017	3.467±.038
-120	2038-H	31	1	3-4	3.6±.5	5.02±.15	.952±.034	1.24 ±.04	.71±.25	<1.9	.228±.018	3.407±.037
-121	2038-J	31	1	14-15	2.6±.6	4.47±.20	1.206±.036	1.13 ±.04	<.8	<1.5	.174±.018	2.962±.033
-174	2045-Y	31	1	26-27	1.2±.4	3.92±.10	1.225±.034	.975±.025	.62±.24	<2.3	.178±.021	2.646±.028
-175	2045-Z	31	1	40-41	6.1±.6	3.22±.12	1.210±.035	.812±.024	<.8	<2.4	.146±.027	2.267±.024
-122	2038-K	31	1	84-85	6.9±.5	3.21±.05	1.280±.039	.921±.04	<.9	<1.4	.100±.015	2.067±.025

1. The sea water contaminations of Na and Mg (as deduced from the Cl abundances) have been removed from the values.

TABLE II

Abundances (expressed in ppm) of elements near the Eocene-Oligocene boundary in DSDP Site 149, which correlate* to some extent with CaCO₃ deposition

NAA P111

Name	Sr	Mn	Cr	Sb	Co	Ni
2038-E	1573±165	2054±41	30.5±1.0	.31±.07	14.85±.18	56±6
2045-X	1520±216	2306±75	31.3±.6	.35±.06	13.66±.23	53±6
2038-F	1209±150	1779±36	38.4±1.0	.42±.09	18.94±.26	76±8
2038-C	260±99	1368±27	34.3±1.2	.33±.11	23.39±.31	86±10
2038-H	296±98	1294±26	34.7±1.2	.38±.11	23.06±.30	98±10
2038-J	262±97	1257±26	36.9±1.2	.42±.11	21.00±.29	103±10
2045-Y	332±114	1153±39	33.5±.8	.46±.09	19.24±.30	93±9
2045-Z	475±132	1477±49	30.6±.8	.41±.08	17.19±.28	77±8
2038-K	478±112	1284±26	28.6±1.0	.42±.10	16.85±.25	75±9

*The elements are arranged in order of decreasing correlation with CaCO₃ deposition.

TABLE III

Abundance (expressed in ppm) of rare earths and Th¹ in DSDP Site 149 near the Eocene-Oligocene boundary

NAA P111

Name	La	Ce ²	Sm	Eu	Tb	Dy	Lu	Th
2038-E	10.47±.27	17.30±.22	2.378±.024	.596±.027	.338±.019	2.33±.14	.216±.013	1.82±.06
2045-X	10.2 ±.6	16.84±.17	2.159±.022	.579±.009	.338±.020	2.47±.16	.199±.013	1.87±.04
2038-F	10.97±.35	19.82±.24	2.652±.027	.70 ±.04	.403±.026	2.75±.15	.225±.017	2.20±.06
2038-G	26.7 ±.5	37.39±.37	6.70 ±.07	1.74 ±.07	1.16 ±.04	6.81±.13	.629±.026	4.86±.09
2038-H	28.1 ±.5	39.09±.39	7.12 ±.07	1.93 ±.07	1.20 ±.04	7.75±.14	.672±.027	5.11±.09
2038-J	27.9 ±.5	37.81±.38	7.22 ±.07	1.84 ±.07	1.25 ±.04	8.18±.14	.665±.028	4.96±.08
2045-Y	32.2 ±.9	39.3±.4	8.02 ±.08	2.079±.021	1.29 ±.04	7.92±.13	.743±.026	5.27±.06
2045-Z	27.7 ±.8	33.78±.34	6.51 ±.07	1.671±.016	1.015±.037	6.88±.14	.600±.023	4.99±.06
2038-K	21.9 ±.4	29.92±.30	5.40 ±.05	1.38 ±.06	.860±.034	6.00±.13	.464±.022	4.05±.07

1. Th may correlate with rare earths because its phosphates are also very insoluble in normal seawater.
2. Ce abundances follow a pattern different from that of other rare earths because rare-earth-containing biogenic components (which reflect the seawater depletion in Ce) may be less abundant in the Oligocene than in the Late Eocene samples.

TABLE IV

Abundances of other trace elements¹ expressed in ppm or (for Ir) in ppb
in DSDP Site 149 near the Eocene-Oligocene boundary

NAA Pill Name	Rb ²	Cs ²	U ²	Ta ²	Hf ³	Sc ³	Zn ⁴	Ir (ppb) ^{4, 5}	Ba
2038-E	19±8	1.02±.06	.357±.015	.1126±.0027	.92±.04	7.90±.08	43.6±2.5	<.36 (-.16±.18)	641±16
2045-X	23.1±3.1	1.31±.08	.411±.024	.0999±.0026	.77±.04	7.58±.08	32.1±3.4	<.21 (.05±.08)	710±16
2038-F	19±6	1.50±.10	.398±.020	.1488±.0032	1.2±.05	10.46±.10	48.8±3.9	<.22 (.02±.10)	757±20
2038-G	28±8	2.12±.13	.752±.024	.343 ±.005	2.13±.06	19.56±.20	299±6	.41±.16	1044±25
2038-H	39±8	2.13±.13	.859±.025	.258 ±.004	2.37±.06	19.58±.20	231±6	.34±.10	936±24
2038-J	21±7	1.87±.12	.711±.025	.201 ±.004	2.10±.06	18.39±.18	157±5	<.42 (.14±.14)	1289±28
2045-Y	34±4	1.75±.12	.652±.034	.1844±.0036	1.78±.06	17.17±.17	177±5	<.34 (.06±.14)	1105±23
2045-Z	28±4	1.58±.11	.681±.032	.1807±.0034	1.62±.06	14.50±.14	125±5	<.24 (-.01±.12)	1399±26
2038-K	22±6	1.57±.11	.509±.022	.156 ±.004	1.39±.05	13.63±.14	78±4	<.26 (-.15±.13)	1138±25

1. Se abundances were all less than 1.1 ppm, and Br abundances, after removing sea water contributions, were all less than 7 ppm.

2. Rb, Cs, Ta and U as well as the major elements Fe, Na and Ti correlate

roughly with Al and may be related to clay (or other aluminium silicate) deposition.

3. Hf and Sc as well as Ce and Th correlate with both Al and the rare earths, and they may be related to both clay (or other aluminum silicate) and biogenic deposition.

4. Zn and Ir do not correlate with any other elements or each other.

5. Flux monitors were used for calibration of abundances. Accuracies are probably ~10-20%.

TABLE V

Major elements abundances (expressed in percent) in samples of
the Permian-Triassic boundary region

Section	Distance above or below base of boundary	Sample No.	NAA Name	Ca	Al	Mg [#]	Fe	Ti	K	Na
Tien Bao	+2 in	38	1091-Q	.69 ±.20	11.9±.1	3.2±.6	1.734±.029	.199±.010	4.42±.15	.0239±.0018
	+5 in	49	1091-Z	.92 ±.17	10.9±.2	2.2±.4	2.129±.032	.214±.009	4.28±.14	.0260±.0018
	+6 in	82	1095-Z	<.4	10.8±.3	2.1±.4	2.256±.033	.208±.010	4.30±.14	.0146±.0016
Triassic samples (all mudstone)										
Tien Bao	+31 ft	51	1091-T	3.86±.33	7.22±.14	1.3±.4	4.27 ±.06	.386±.013	2.96±.17	.2495±.0036
	+8 ft 8 in	42	1091-R	3.77±.29	7.66±.11	3.2±.5	3.42 ±.05	.381±.012	3.67±.17	.1380±.0030
	+6.5 in	48	1091-Y	3.75±.30	7.71±.12	1.8±.4	3.48 ±.05	.361±.013	3.38±.15	.1842±.0029
	+5 in	39	1091-V	1.96±.25	8.47±.09	2.2±.6	2.625±.039	.408±.011	3.71±.15	.1245±.0026
Permian samples (all shale except no. 52 which is unknown)										
Tien Bao	-4 in	50	1095-X	28.7±.8	2.15±.09	.80±.35	1.130±.019	.054±.039	1.21±.17	.0467±.0029
Wachapo Mtn.	-2 in	80	1095-Y	.47±.11	7.37±.17	.96±.34	1.085±.019	.174±.009	2.07±.09	.0293±.0014
Tien Bao	-?*	46	1091-U	24.5±.7	2.54±.09	.63±.27	.727±.016	.029±.024	.64±.06	.0568±.0015
	-7.5 ft 2 in	45	1091-X	6.66±.33	8.16±.11	<.10	1.636±.026	.081±.012	2.22±.10	.0405±.0016
	-7-27 ft-2 in	47	1091-S	21.5±.6	1.20±.05	.82±.25	1.104±.020	.042±.021	.34±.06	.0338±.0013
	-?*	52	1091-W	2.38±.24	11.44±.13	<1.6	2.492±.037	.307±.010	2.83±.11	.0858±.0019

Flux monitor was used for the abundance calibration.

* This sample comes from 7ft 3in above the brownish layer separating the Upper and Lower Changhsing Formation.

Its exact position with respect to the boundary is not known.

** This sample comes from a 2in thick bed in the Changhsing Formation 20ft above the top of the underlying Longtan Formation.

TABLE VI

Trace element abundances expressed in ppm (ppb for Ir) in samples of the Permian-Triassic boundary region

Sample	Ba	Co	Cr	Cs	Eu	Hf	In*	Ir(ppb)	Mn
Boundary Layer									
38	<63	4.41±.14	<2.7	31.4 ±.4	1.465±.018	14.36±.16	.147±.022	<.4	59.4±1.2
49	<42	1.20±.10	2.5±.8	34.8 ±.5	1.185±.016	12.92±.15	.070±.029	<.1.5	45.4±.9
82	64±32	6.06±.16	<1.8	12.38±.20	2.247±.021	11.46±.13	.148±.029	<.5	15.0±.4
Triassic Samples									
51	287±15	25.55±.38	66.6±1.3	10.23±.18	1.073±.014	4.34±.08	<.18	<.4	433±9
42	347±14	25.74±.4	69.1±1.4	10.76±.19	.972±.013	4.61±.08	<.11	<.5	354±7
48	307±16	14.06±.25	97.6±1.4	13.28±.22	1.04±.06	4.92±.09	<.14	<2.2	189.5±3.8
39	337±16	15.09±.27	99.8±1.5	12.57±.21	1.44±.08	5.23±.09	<.11	<.9	160.8±3.2
Permian Samples									
50	61±10	3.86±.11	59.6±.8	2.77±.09	.83±.05	1.53±.05	<.14	<.28	77.3±1.6
80	91±10	6.12±.15	20.8±.8	8.84±.15	1.111±.013	4.62±.07	.049±.023	<.21	25.6±.5
46	86±18	3.68±.12	84.6±1.2	2.82±.09	1.28±.06	1.76±.07	.054±.026	<.18	67.5±1.3
45	48±13	4.30±.13	67.8±1.0	7.25±.13	.291±.034	4.16±.08	<.05	<.33	65.2±1.3
47	90±11	4.29±.12	84.5±1.0	1.68±.08	.390±.034	1.05±.05	<.04	<.30	72.4±1.4
52	82±11	.39±.09	119.4±1.5	14.01±.22	.556±.010	8.11±.10	.066±.018	<.24	14.4±.5

TABLE VI (continued)

Sample No.	Ni	Rb	Sb	Se*	Sm	Ta	Th	U	V
Boundary Layer									
38	19±5	144±7	1.45±.13	3.57±.39	13.12±.13	2.228±.022	59.6±.6	7.02±.05	<50
49	<27	135±6	2.06±.15	2.82±.37	10.71±.11	2.037±.020	48.3±.5	5.79±.05	<54
82	20±6	178±7	.42±.08	<.6	16.30±.16	1.816±.018	46.4±.5	5.04±.06	<66
Triassic Samples									
51	67±9	143±7	2.53±.18	.76±.31	5.64±.06	.967±.010	14.91±.15	3.494±.035	113±17
42	49±9	146±8	.76±.11	<.8	5.16±.05	1.017±.010	14.52±.15	3.265±.031	146±16
48	63±9	162±7	3.59±.23	6.33±.35	6.25±.06	1.075±.011	19.40±.19	6.79±.05	144±17
39	61±9	160±7	3.36±.22	5.16±.34	8.99±.09	1.178±.012	21.43±.21	7.56±.05	155±16
Permian Samples									
50	40±4	36.3±2.5	1.91±.13	6.90±.23	4.53±.05	.3005±.0035	6.13±.05	8.89±.09	46±15
80	<23	90±4	.46±.07	<.4	8.35±.08	1.063±.011	16.9±.9	4.95±.05	<53
46	43±5	36.7±3.2	1.08±.10	12.49±.35	8.58±.09	.471±.005	12.67±.13	38.43±.38	80±12
45	38±6	119±5	2.37±.16	18.40±.37	2.508±.025	.978±.010	26.90±.27	7.95±.08	89±14
47	80±5	27.5±2.4	1.42±.11	28.41±.38	1.566±.016	.2408±.0036	3.59±.04	12.57±.13	139±11
52	79±8	128±6	3.69±.23	.91±.27	3.326±.033	.882±.009	17.25±.17	11.00±.11	120±17

* Flux monitors were used for calibration of abundances. Accuracies are probably ~10-20%.

This report was done with support from the Department of Energy. Any conclusions or opinions expressed in this report represent solely those of the author(s) and not necessarily those of The Regents of the University of California, the Lawrence Berkeley Laboratory or the Department of Energy.

Reference to a company or product name does not imply approval or recommendation of the product by the University of California or the U.S. Department of Energy to the exclusion of others that may be suitable.

TECHNICAL INFORMATION DEPARTMENT
LAWRENCE BERKELEY LABORATORY
UNIVERSITY OF CALIFORNIA
BERKELEY, CALIFORNIA 94720